

RESEARCH ARTICLE

Microstrip array antenna bandwidth enhancement using reactive surface

Arun Bhattacharyya  | Dooheon Yang | Sangwook Nam

Electrical Engineering Department, Seoul National University, Gwanak-gu, Republic of Korea

Correspondence

Arun Bhattacharyya, Electrical Engineering Department, Seoul National University, Gwanak-gu, Republic of Korea.

Email: arun.k.bhattacharyya@lmc.com

Present address

Arun Bhattacharyya, Lockheed Martin Space Systems, RF Center of Excellence, Littleton, CO 80125.

Funding information

This research was supported by Brain Pool program funded by the Ministry of Science and ICT through the National Research Foundation of Korea (2018H1D3A2001827), Grant/Award Number: 2018H1D3A2001827

Abstract

A single layer reactive screen, made of printed elements, is introduced to increase the bandwidth of a patch array antenna. It is found that by decreasing the periodicity of the printed elements on the screen, the return loss bandwidth can be improved significantly compared with a two-layered stacked patch counterpart. Simulated results are shown, and the bandwidth improvements are explained in terms of a standard stub-matching procedure that is normally exercised in microwave circuits.

KEYWORDS

bandwidth improvement, patch array, probe-fed patch, reactive screen

1 | INTRODUCTION

For air-borne and space applications, the microstrip patch array antenna is preferred due to its low profile and light weight.

The work was conducted at Electrical Engineering Department, Seoul National University, Gwanak-gu, Republic of Korea.

However, in many situations, the narrow bandwidth characteristic of a patch element prohibits from using it. The bandwidth of a patch element increases in the array environment when the element spacing is low. Thus, for a given aperture size the number of elements should be large to take advantage of the proximity coupling. A larger number of elements drive up the cost of an array as the number of active elements, such as solid-state power amplifiers and phase shifters, need to be increased subsequently. For a moderate scan requirement, the element spacing need not be small. Hence, a wide-band patch solution for moderate element spacing is desirable.

Several methods are reported in the literature to increase the bandwidth of patch elements.¹⁻⁸ The simplest one, particularly for array application, perhaps, using another layer of passive patch-elements. The resonance of the passive patches is used favorably to enhance the overall bandwidth. The reactive impedance screens (RIS) are also employed primarily for miniaturizing the size of an isolated radiating element and, in some cases, for bandwidth enhancement.⁵⁻⁸ In Reference 5 Mosallaei and Sarabandi demonstrated that a very compact patch on a RIS structure can have 6.7% bandwidth. Similar studies were conducted by other researchers⁶⁻⁸ with an objective to improve impedance bandwidth and axial ratio bandwidth. In the above cases, the RIS was placed underneath the driven patch element. In Reference 9 a single truncated-corner square patch radiator loaded with an RIS above the driven patch was studied and a significantly wide band performance (~45%) is reported. Such a bandwidth enhancement was achievable due to the direct radiation of the surface wave mode through the truncated edge of the dielectric substrate. For an array antenna, the above principle does not apply because (a) a surface wave propagation is not desirable as it causes scan blindness, and (b) a truncated dielectric edge does not exist in the array environment. In other words, in the array environment, the characteristics of the element presented in Reference 5 will not exhibit the same bandwidth characteristics.

In this article we propose a reactive surface (RS) loaded patch array to enhance the array-bandwidth while keeping a moderate element spacing. The conventional stacked patch array can be viewed as the RS loaded patch array as the stacked patch layer offers a reactive impedance to the driven patch layer. However, it is found that the upper end of the band is limited by the stacked patch layer that acts as a frequency selective surface (FSS), having an upper cutoff frequency.¹⁰ Clearly, by stretching the cutoff frequency of the upper layer, the bandwidth can be increased; one of the ways to accomplish is to decrease the periodicity of the upper layer elements. We show conceptually and with rigorous numerical

simulations that by decreasing the periodicity of printed elements on the RS layer the bandwidth can be increased significantly. The effects of higher order Floquet modal interactions with the driven patch layer can be compensated by adjusting the offset distance of the RS layer. We present a design guideline of such an array using a simple “stub-matching” method that is commonly employed in microwave circuit arena. We also display numerical results for the reflection coefficients and demonstrate the bandwidth enhancement in comparison with the stacked patch array counterpart. The scan performance and the active element patterns are also shown.

1.1 | ANALYSIS

Figure 1 shows an exploded view of a probe-fed patch array loaded with an RS screen. The RS consists of an array of printed patch metallization. Unlike a stacked patch array, the periodicity of the RS is different from that of the driven patch elements. The unit cell size of the driven patch is assumed as $a_1 \times b_1$, and the substrate thickness is h_1 . The spacer thickness between the driven patch and the RS is h_2 and the cell size for the elements of RS is $a \times b$. For a rigorous analysis of such a structure with different periodicities of the layers, we should invoke the procedure detailed in Reference 11. For analytical simplicity, we consider that the periodicity of the RS is half of the driven patch layer (ie, $a = a_1/2$ and $b = b_1/2$) in each direction. In other words, a unit cell of a driven patch accommodates four elements of RS as shown in Figure 1.

A unit cell of the probe-fed patch layer can be represented by a multimodal admittance matrix [Reference 11(p228)]. However, it is complicated to have a physical equivalent circuit representing input and output modal quantities primarily due to unequal number of modes of probe and patch and non-symmetrical nature of the admittance-matrix for a general Floquet excitation. Furthermore, the higher order Floquet

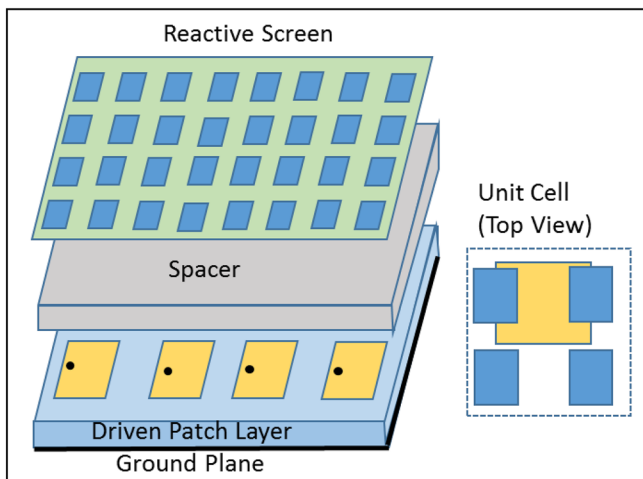


FIGURE 1 Schematic of a patch array loaded with a reactive screen. The overall unit cell of the array is also shown [Color figure can be viewed at wileyonlinelibrary.com]

modes cannot be ignored in the admittance matrix formulation as they are responsible for energy stored in the near field region. To alleviate the problems, we analyze the structure from the aperture side, that is, in the “receiving antenna” mode. From the aperture side the patch array is equivalent to a complex admittance surface with respect to a plane wave incident on the array aperture. For the dominant Floquet incident mode from aperture side, the lumped surface admittance is given by

$$Y_p = \frac{1 + S_{22}(n, n)}{1 - S_{22}(n, n)} \quad (1)$$

where $S_{22}(n, n)$ represents the element of the generalized scattering submatrix $[S_{22}]$ associated with the dominant Floquet mode incident upon the patch layer. Depending on the incident polarization, the dominant Floquet mode could be either TE or TM type. The above lumped admittance is the normalized admittance with respect to the Floquet modal admittance of the dominant mode under consideration. For $Y_p = 1$, the antenna is perfectly matched with the incident Floquet mode. If this condition is satisfied, then from reciprocity, the antenna is perfectly matched from the input side, under the assumption that the array does not have any grating lobe, which is generally true for boresight radiation or for a small scan requirement. We will examine the admittance behavior of a typical patch array in the receiving mode.

1.2 | Patch surface admittance

The generalized scattering matrix of a single layer probe-fed patch is analyzed using a “Floquet Method of Moment (MoM)” analysis.¹² The lumped surface admittance from the aperture side is extracted for the normal incidence using Equation (1). Figure 2 shows the real and the imaginary parts of the admittance with respect to two reference planes,

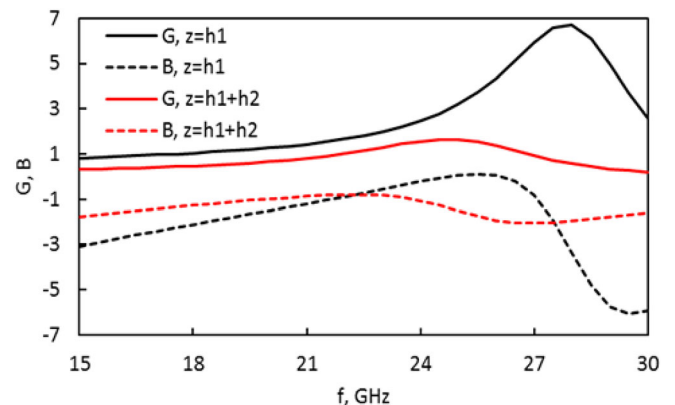


FIGURE 2 The complex admittance of a probe-fed patch looking from aperture side. The feed line is terminated by 50 Ohms load. The dimensions are: $a_1 = b_1 = 0.8$ cm, patch sizes = 0.43 cm \times 0.43 cm, $h_1 = 0.0734$ cm, $h_2 = 0.0647$ cm. Probe diameter = 0.05 cm. Probe location 0.04 cm from edge [Color figure can be viewed at wileyonlinelibrary.com]

one of which is just above the patch surface and the other is at a distance h_2 above the patch surface. The mid-frequency of the desired operating band is 22.5 GHz and the element spacing is 0.8 cm (about $0.6\lambda_0$, where λ_0 is the free-space wavelength at the mid-frequency). For the reference plane just above the patch surface, the output conductance G and output susceptance B vary widely with frequency near 27 GHz. However, the variation is much contained when the reference plane is moved at a distance h_2 above the patch surface. Furthermore, the conductance G is near unity over a wide frequency range. However, a moderately large offset inductive reactance is observed. Thus, using the concept of “stub-matching” a capacitive reactance surface will neutralize the inductive reactance yielding a good impedance match in the receiving mode. As the intrinsic reactance at the reference plane is almost flat, the RS that has a similar “flat” behavior with frequency is desired. It is well known that a printed patch surface behaves as a low pass spatial filter that exhibits a capacitive reactance at a low frequency. However, beyond the cutoff frequency, the patch surface becomes inductive. The cutoff frequency can be controlled by changing the periodicity of the printed elements.

Figure 3 shows the equivalent shunt susceptances of two reactive surfaces made of rectangular patch elements with two different periodicities (solid line curves). For the RS having the same periodicity of the driven patches (ie, $a = b = 0.8$ cm, we call RS-1), the susceptance at the upper end of the band varies exponentially as the frequency approaches toward the cutoff point. However, when the periodicity is reduced to 0.4 cm (we call RS-2), the susceptance shows a very gradual variation as the cutoff frequency is far above 30 GHz. The total susceptance (ie, Patch + RS) is also plotted in the same figure. The total susceptance using the screen of lower periodicity (RS-2) shows a characteristic

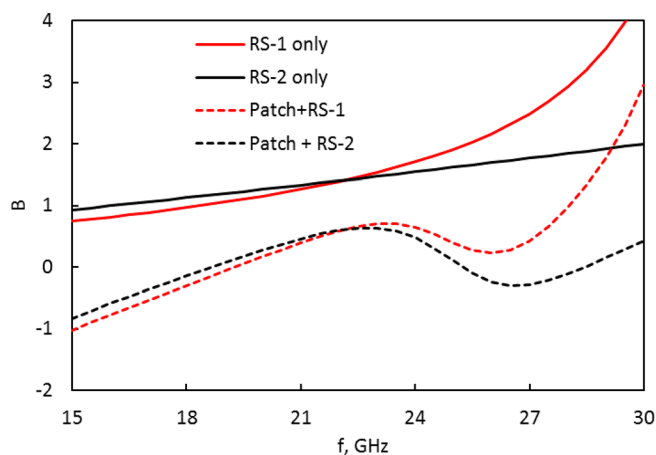


FIGURE 3 Susceptance of the reactive screen layer. Also shown susceptance of the patch layer and screen layer together from aperture side. Patch dimensions are same as in Figure 2. The screen layer RS-1 has a cell dimension of 0.8 cm \times 0.8 cm. The cell dimension of RS-2 is 0.4 cm \times 0.4 cm. The dielectric constant of spacer is 1.1 [Color figure can be viewed at wileyonlinelibrary.com]

favorable for wide-band performance. The dimension of the RS patch elements can be adjusted to obtain the appropriate magnitude of the susceptance.

2 | RESULTS

The foregoing analysis suggests that a RS can enhance the operating bandwidth of a patch array. This is not surprising as it is well established that a stacked patch array shows wider bandwidth than that of a single layer patch array. What is interesting here is that *by increasing the number of passive stacked elements it is possible to stretch the bandwidth, while keeping the periodicity of the driven patch unchanged*. Increment of patch elements on the upper layer does not create much fabrication issue. Based on the above principle, we optimized four patch arrays and compared their performances. For optimization, the empirical data based on the “stub-matching” method described earlier was used as the trial solution. For a fair comparison, the substrate thickness of the driven patch is kept identical for all four cases. The performances were optimized using a gradient search optimizer and the main analysis engine was a Floquet (MoM) model¹² for fast optimization. The generalized scattering matrix approach was invoked, and the layers were analyzed independently and then cascaded.¹² For good convergence, the number of basis-functions were over 350 on a single patch and the number of Floquet modes were over 1500. To handle different periodicities of the layers, the analytical method presented in Reference 11 was employed. The dimensions of the driven patch and the patch on the RS layer, the spacer thickness and the offset of the RS layer were optimized for the best bandwidth performance.

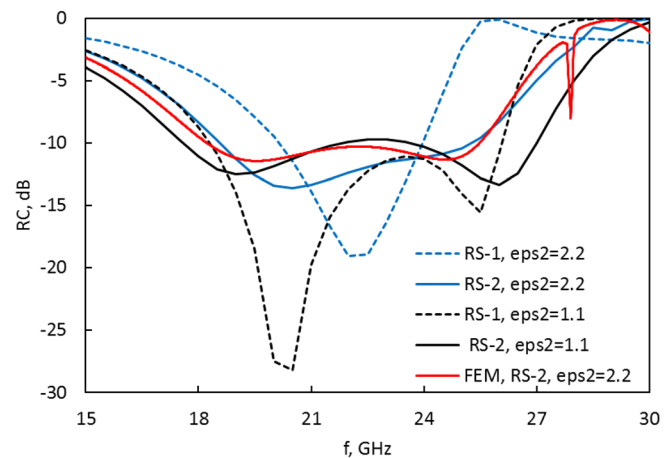


FIGURE 4 Input reflection coefficients of four patch arrays loaded with reactive surfaces. The patch dimensions are optimized for the best performance. The parameters are: $a_1 = b_1 = 0.8$ cm, $h_1 = 0.0734$ cm, feed probe diameter = 0.05 cm, probe location 0.04 cm from patch edge. ---- $L = 0.404$ cm, ____ $L = 0.392$ cm, ----- $L = 0.460$ cm, _____ $L = 0.430$ cm, _____ $L = 0.392$, $L =$ patch length of driven square patches [Color figure can be viewed at wileyonlinelibrary.com]

Figure 4 shows the reflection coefficients of four patch arrays loaded with reactive screens. The dash lines (labeled by RS-1 at the inset) correspond to the screens that have identical periodicity with that of the driven patch (like the conventional stacked patches). The solid lines (labeled by RS-2 at the inset) are with screens that have half the periodicity of the driven patches. For the best performance, the RS-2 screen is offset about half of its periodicity on E-plane as displayed in Figure 1. As can be noted, screens with smaller periodicities significantly improve the bandwidths. For instance, the stacked patch (ie, with 0.8 cm screen periodicity) with spacer's dielectric constant of 2.2 ($\epsilon_{s2} = 2.2$) has about 18% bandwidth correspond to 10 dB return loss. When the screen periodicity reduces to 0.4 cm, the bandwidth increases to 32%. This is a significant bandwidth improvement. For lower dielectric constant of the spacer ($\epsilon_{s2} = 1.1$) the bandwidth is 37% for a stacked patch, which improves to 42% for the screen loaded (RS-2) patch array counterpart. For the lower dielectric spacer case the improvement is not too high because the cutoff frequency of the RS screen on low dielectric material is naturally higher even for $a = 0.8$ cm. For high-frequency application, use of a low dielectric material (Rohacel, for example) may have an issue due to the large fabrication tolerance, but for low frequency application that is not an issue. The numerical result for high-dielectric spacer case is compared with that obtained using a commercial finite element method simulation and the result matches with the MoM method used in the present analysis.

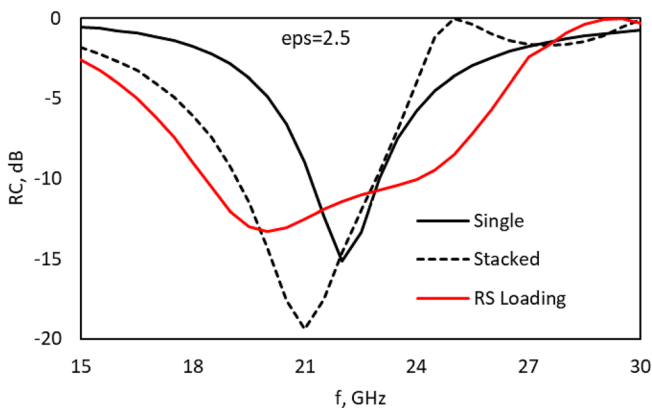


FIGURE 5 Reflection coefficients of single layer, stacked, and reactive screen loaded square patch arrays. The dielectric constant is 2.5 and lower layer and upper layer thicknesses are 0.0734 cm and 0.0793 cm, respectively. Patch length $L = 0.3923$ cm for the single layer. For the staked patch, $L = 0.3923$ cm (lower layer), $L = 0.2908$ cm (upper layer). For the RS loaded patch, $L = 0.3758$ cm. The RS is made of offset printed square elements of length 0.2365 cm, with periodicity 0.4 cm. The patch periodicity is 0.8 cm in both directions. The patches are excited by probe of diameter 0.05 cm, located at 0.04 cm from the edge [Color figure can be viewed at wileyonlinelibrary.com]

Figure 5 compares the reperformances three patch array configurations, namely (a) single layer patch array, (b) two-layer stacked patch array, and (c) single layer patch array loaded with reactive screen. The patch periodicity for all three cases is 0.8 cm in both directions. For the reactive layer, the periodicity of the printed square elements is 0.4 cm in both directions. The dielectric constant of the layers is 2.5. We optimized patch dimensions to obtain the best performances for the stacked patch array and the reactive screen loaded patch array. For a fair comparison, the thicknesses of the dielectric layers are kept identical. Note that the reactive screen loaded patch shows improved bandwidth performance as compared with the stacked-patch array counterpart. In this design example, the -10 dB reflection coefficient bandwidths for stacked patch and reactive screen loaded patch are 18% and 28%, respectively. The single layer patch array shows about 9% bandwidth.

In Figure 6 we plot the scan performance of the RS screen loaded array. For this case we used the reactive screens (RS-2 of Figure 4) that have smaller periodicities as compared with that of the driven patches. As noted, the reflection coefficient deteriorates as the scan angle approaches to the blind spot. This behavior is very similar that of a regular patch array of similar periodicity. Within 25° scan-angle, the impedance match is reasonably good.

For a scan array design consideration, the blind angle of an RS loaded patch array can be determined analytically. The blind angle is primarily due to the lowest order TM surface wave mode supported by the array structure. On the principal planes, one can estimate the blind angles using the following relation in reference11(p103):

$$k_0 \sin \theta_b + k_{ps} = \frac{2\pi}{a_1}, \quad (2)$$

where k_0 is the wave number in free space, θ_b is the blind angle, k_{ps} is the surface wave number, and a_1 is the patch-

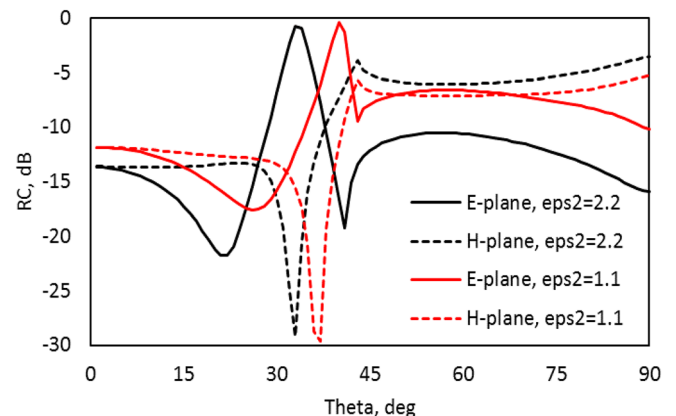


FIGURE 6 Reflection coefficient vs scan angle at 22.5 GHz for the patches loaded with RS-2. The dielectric constant of the bottom layer is 2.2. The dielectric constants of the upper layer (superstrate) are 2.2 and 1.1 for two cases. The other parameters are given in Figure 4 [Color figure can be viewed at wileyonlinelibrary.com]

periodicity. The surface wave number for small substrate thickness can be approximated as¹²

$$k_{ps} \approx k_0 \left[1 + \frac{1}{2} \left\{ k_0 h \left(1 - \frac{1}{\epsilon_r} \right) \right\}^2 \right]. \quad (3)$$

In Equation (3), h is the substrate thickness and ϵ_r is the dielectric constant of the substrate. For the RS loaded patch array, the superstrate effect must be included in the analysis. If the substrate and superstrate have identical dielectric material ($\epsilon_{ps} = 2.2$ case in Figure 6), then one can use the total dielectric thickness as h (ie, $h = h_1 + h_2$). We use $\epsilon_r = 2.2$, $a_1 = 0.8$ cm, $h = 0.1507$ cm ($=h_1 + h_2$), $f = 22.5$ GHz in Equations (2) and (3) and obtain the blind angle as $\theta_b = 36^\circ$, which agrees with that in Figure 6. We emphasize here that that Equation (3) is valid if the two layers have identical dielectric constant. For the “ $\epsilon_{ps} = 1.1$ ” case of Figure 6, one can ignore the upper layer (because of low ϵ_r , which is close to air) and use Equation (3) for the surface wave number and estimate the blind angle. Using $h = 0.0734$ cm, and keeping the other parameters unchanged, we obtain the blind angle at about 40° . This result also agrees with that in Figure 6 ($\epsilon_{ps} = 1.1$ case). It should be mentioned that the patch metallization has some effects on the surface wave number, which is ignored in our analysis. For the present situation the “patch metallization effect” is negligible because of large periodicity compared with the patch dimensions.

3 | CONCLUSIONS

We have shown that a patch array loaded with a reactive screen improves the bandwidth significantly. The improvement is substantial if the periodicity of the printed elements on the screen is reduced. Numerical simulation indicates that the 10 dB return loss bandwidth improves from 18% to 32% if four printed elements, instead of one, on the RS are used within a unit cell of the driven patch. This particular bandwidth enhancement method is useful for a low-cost array design where the element spacing is not constrained by wide angle scan requirement.

ORCID

Arun Bhattacharyya  <https://orcid.org/0000-0002-8845-401X>

REFERENCES

- [1] Sun C, Zheng H, Zhang L, Liu Y. Analysis and design of a novel coupled shorting strip for compact patch antenna with bandwidth enhancement. *IEEE Antennas Wirel Propag Lett.* 2014;13:1477-1481.
- [2] Liu Y, Shafai L, Shafai C. Gain and bandwidth enhancement of stacked H shaped patch-open ring antenna, 17th International Symposium on Antenna Technology and Applied Electromagnetics (ANTEM), 2016.
- [3] Yasin T, Baktur R. Bandwidth enhancement of meshed patch antennas through proximity coupling. *IEEE Antennas Wirel Propag Lett.* 2017;16:2501-2504.
- [4] Asaadi M, Sebak A. Gain and bandwidth enhancement of 2×2 square dense dielectric patch antenna array using a holey superstrate. *IEEE Antennas Wirel Propag Lett.* 2017;16:1808-1811.
- [5] Mosallaei H, Sarabandi K. Antenna miniaturization and bandwidth enhancement using a reactive impedance substrate. *IEEE Trans Antennas Propagat.* 2004;52(9):2403-2414.
- [6] Costa F, Luukkonen O, Simovski CR, Monorchio A, Tretyakov SA, de Maagt PM. TE surface wave resonances on high-impedance surface based antennas: analysis and modeling. *IEEE Trans Antennas Propagat.* 2011;59(10):3588-3596.
- [7] Bernard L, Chertier G, Sauleau R. Wideband circularly polarized patch antennas on reactive impedance substrates. *IEEE Antennas Wirel Propag Lett.* 2011;10:1015-1018.
- [8] K. Agarwal, Nasimuddin and A. Alphones, “RIS-based compact circularly polarized microstrip antennas,” *IEEE Trans Antennas Propagat* Vol. 61, No. 2, pp. 547–554, 2013.
- [9] Ta SX, Park I. Low-profile broadband circularly polarized patch antenna using metasurface. *IEEE Trans Antennas Propagat.* 2015;63(12):5929-5934.
- [10] Bhattacharyya AK. Bandwidth limits of multilayer array of patches excited with single and dual probes and with a shorting post. *IEEE Trans Antennas Propagat.* 2011;59(3):818-825.
- [11] Bhattacharyya AK. Analysis of multilayer infinite periodic array structures with different periodicities and axes orientations. *IEEE Trans Antennas Propagat.* 2000;48(3):357-369.
- [12] Bhattacharyya AK. *Phased Array Antennas- Floquet Analysis, Synthesis, BFNs and Active Array Systems.* Hoboken, New Jersey: Wiley; 2006.

How to cite this article: Bhattacharyya A, Yang D, Nam S. Microstrip array antenna bandwidth enhancement using reactive surface. *Microw Opt Technol Lett.* 2020;62:825–829. <https://doi.org/10.1002/mop.32081>